



## Analysis of Diurnal and Seasonal Variation of Submicron Outdoor Aerosol Mass and Size Distribution in a Northern Indian City and Its Correlation to Black Carbon

S.P. Baxla<sup>1</sup>, A.A. Roy<sup>1</sup>, Tarun Gupta<sup>1\*</sup>, S.N. Tripathi<sup>1</sup>, R. Bandyopadhyaya<sup>2†</sup>

<sup>1</sup> Department of Civil Engineering, Environmental Engineering Programme, Indian Institute of Technology Kanpur, Kanpur 208016, India

<sup>2</sup> Department of Chemical Engineering, Indian Institute of Technology Kanpur, Kanpur 208016, India

### ABSTRACT

The seasonal and diurnal behavior of atmospheric submicron aerosol was studied in the northern Indian city of Kanpur in the Indo Gangetic Plain during July 2006–May 2007. The size distribution and mass concentration of the aerosol in the range of 15–700 nm was measured using a scanning mobility particle sizer (SMPS). Simultaneously, black carbon (BC) measurement was made using an aethalometer. The measurements were recorded for four different seasons, viz. monsoon, post-monsoon, winter and pre-monsoon. The diurnal variation of BC and submicron aerosol mass followed very similar trends in all the seasons. This is evident by the fact that BC had strong positive correlation with the submicron aerosol mass ( $0.83 \leq R \leq 0.96$ , where R is the Pearson's correlation coefficient). Both peaked once in the morning [07:00–09:00 local time (LT)], and once in the night (20:00–22:00 LT). The peak concentrations varied from season to season, which could be attributed to seasonal variation in anthropogenic activity, traffic movement and atmospheric boundary layer conditions. The background aerosol number concentration in winter ( $\sim 10^5 \text{ \#/cm}^3$ ) was an order of magnitude higher than that observed in other seasons ( $\sim 10^4 \text{ \#/cm}^3$ ); and on a foggy day in the winter, it was twice as high as that seen on a clear winter day. The fraction ( $F_{BC}$ ) of the BC mass concentration in the submicron aerosol was observed to be highest in monsoon ( $0.18 \pm 0.13$ ), followed by pre-monsoon ( $0.08 \pm 0.02$ ) and post-monsoon ( $0.05 \pm 0.01$ ), with the lowest in winter ( $0.03 \pm 0.01$ ).

**Keywords:** Submicron aerosol; SMPS; Black carbon; Kanpur; Outdoor monitoring.

### INTRODUCTION

Atmospheric aerosols stimulate strong research interest primarily due to their importance in influencing climate, restricting visibility and causing deleterious effects on human health. The aerosol effect on climate is very complex, and depends on several microphysical properties, such as composition, size distribution, hygroscopic behavior and other properties (Jacobson, 2001). Particle size is one of the key parameters regarding atmospheric aerosol transport, subsequent removal (DeReus *et al.*, 2001) and climatology. For a typical urban environment, the submicron range of diameter ( $d_p \leq 1 \mu\text{m}$ ) includes 99.99 % of the total number of particles and 60 % of the total aerosol mass (Whitby *et al.*, 1972). Further the submicron range is divided into the ultrafine ( $d_p \leq 0.1 \mu\text{m}$ ) and accumulation ( $0.1 \mu\text{m} \leq d_p \leq 2.5 \mu\text{m}$ ) range (Seinfeld and Pandis, 1998; Friedlander, 2000). These two ranges are collectively called as the fine aerosol. The primary part of the fine aerosol comprises of black carbon and high molecular weight compounds emitted from combustion sources (Friedlander, 2000). The secondary part

consists of sulfate, nitrate, and aerosols formed from organic vapour precursors (Friedlander, 2000). The higher end of the size range of these particles is of the same order of magnitude as the wavelength of visible light and thereby affects atmospheric visibility (Hinds, 1999). Therefore, an increasing emphasis is being given to the measurement and interpretation of particle size distribution of submicron particles in the atmosphere (Baron and Willeke, 2001).

Elemental carbon and high molecular weight organic compounds directly emitted from combustion processes such as industrial pollution, traffic, outdoor fires, household burning of coal and biomass fuel (Gatari and Boman, 2003; Venkataraman *et al.*, 2005) give rise to fine particles (diameter  $< 1 \mu\text{m}$ ) These particles are known absorbers of solar radiation, reducing the solar radiation coming to earth (Bond and Bergstrom, 2006) by as much as 20–25% (Hermann and Hanel, 1997).

Several field experiments and campaigns have been conducted worldwide in order to recognize the major atmospheric aerosol sources, and the seasonal and diurnal variation of the aerosol size distribution (e.g., Bhugwant *et al.*, 2001; Kuhlbusch *et al.*, 2001; Hussein *et al.*, 2006; Kondo, 2006). The study of the aerosol particles and their characteristics have only recently been investigated in different parts of India, covering urban (Babu *et al.*, 2002; Tripathi *et al.*, 2005; Rana *et al.*, 2009), coastal and continental (Moorthy *et al.*, 2005; Kothai *et al.*, 2008) and oceanic regions (Vinoj *et al.*, 2004; Satheesh *et al.*, 2006).

Encompassing a vast area (21.75°N and 74.25°E to 31.0°N and 91.5°E) and occupying 21% of the Indian subcontinent, the Indo Gangetic Plain (IGP) accounts for approximately 40% of the Indian population (Nair *et al.*, 2007). This area is highly industrialized, and has a cluster of thermal power plants (Prasad

\* Corresponding author. Tel.: +91-512-259 7128;

Fax: +91-512-259 7395

E-mail address: tarun@iitk.ac.in (T. Gupta),

snt@iitk.ac.in (S.N.Tripathi), rajdip@che.iitb.ac.in (R.

Bandyopadhyaya).

† Present address: Department of Chemical Engineering, Indian Institute of Technology, Bombay, Powai, Mumbai 400 076, India.

et al., 2006), small and medium industries, which are amongst the main contributors of particulate matter in this region (Fig. 1). In a polluted city such as Kanpur situated in the IGP, a wide variety of compounds are released into the atmosphere, which may alter the aerosol characteristics and seasonal behaviour. For example there are frequent dust storms in the summer season, which contain absorbing minerals (Dey et al., 2004). As we move towards winter, we see an increase in anthropogenic activity primarily due to heating purposes, which increases the black carbon load.

Ganguly et al. (2006) measured the number and size distribution of near surface aerosols in Delhi during the ISRO Geosphere Biosphere Program Land Campaign II (LC II) in December 2004, observing some spectacular features in the behaviour of aerosol parameters during the clear, foggy and hazy days. The diurnally averaged BC mass concentration reached a high of about  $65 \mu\text{g}/\text{m}^3$  on hazy days, falling to a low of  $15 \mu\text{g}/\text{m}^3$  on clear days. Nair et al. (2007) measured the black carbon (BC) and total aerosol mass concentration over the cities of Kharagpur, Allahabad and Kanpur during LC II, finding the average mass concentrations of total aerosols to be in the range of  $260\text{--}300 \mu\text{g}/\text{m}^3$ , and that of black carbon to be between  $20\text{--}30 \mu\text{g}/\text{m}^3$ . They observed that the dynamics of the local atmospheric boundary layer as well as changes in local emissions affected the diurnal variations of aerosol and black carbon concentrations. It was observed that the aerosol and black carbon mass concentrations correlated inversely with the boundary layer thickness. Satellite (Chu et al., 2003; Ramanathan and Ramana, 2005) and ground-based observations (Mönkkönen et al., 2004; Singh et al., 2004; Dey et al., 2005) have indicated a high aerosol loading over the Ganga basin.

Amongst the factors affecting the aerosol particle number and

mass densities in the urban environment, of particular importance are meteorological parameters such as temperature, relative humidity (RH), wind speed, and hour of the day (Hussein et al., 2006), and also proximity to source as well as removal mechanisms. It also depends upon the atmospheric boundary layer conditions, which in turn experience a very prominent diurnal variation (Tripathi et al., 2005; Tripathi et al., 2007).

Several recent studies have tried to identify and quantify the sources for carbonaceous and mineral aerosol in this part of the World (Srivastava et al., 2008; Zhang et al., 2008). In addition, Tripathi et al. (2006) and Ahammed et al. (2007) have measured the size distribution of the aerosol particles during winter season over Delhi and Kanpur, respectively, using optical particle counters. Ahammed et al. (2007) reported that the number concentration of the aerosol particles on foggy days were approximately thrice higher vis-à-vis those observed on non-foggy days.

Although several detailed atmospheric measurements have been carried out in this region, none has focused on ultrafine aerosols. The ultrafine aerosols are generally composed of local combustion emissions, or particles resulting from atmospheric photochemical activity. These processes give rise to homogenous nucleation and subsequent growth, resulting in particles of sizes upto 100 nm. These particles attach to larger particles which then fall into the size window of 100-1000 nm. They have the maximum residence times in the atmosphere. Although ultrafine particles contribute negligibly to the total aerosol mass (Oberdoster, 2001), they are very high in number, and can cause acute lung injury. It has also been hypothesized that they may contribute to increased mortality and morbidity (Oberdoster et al., 1995). The aim of our work was to explore the seasonal and diurnal variation of (1) ultrafine and accumulation particles' mass

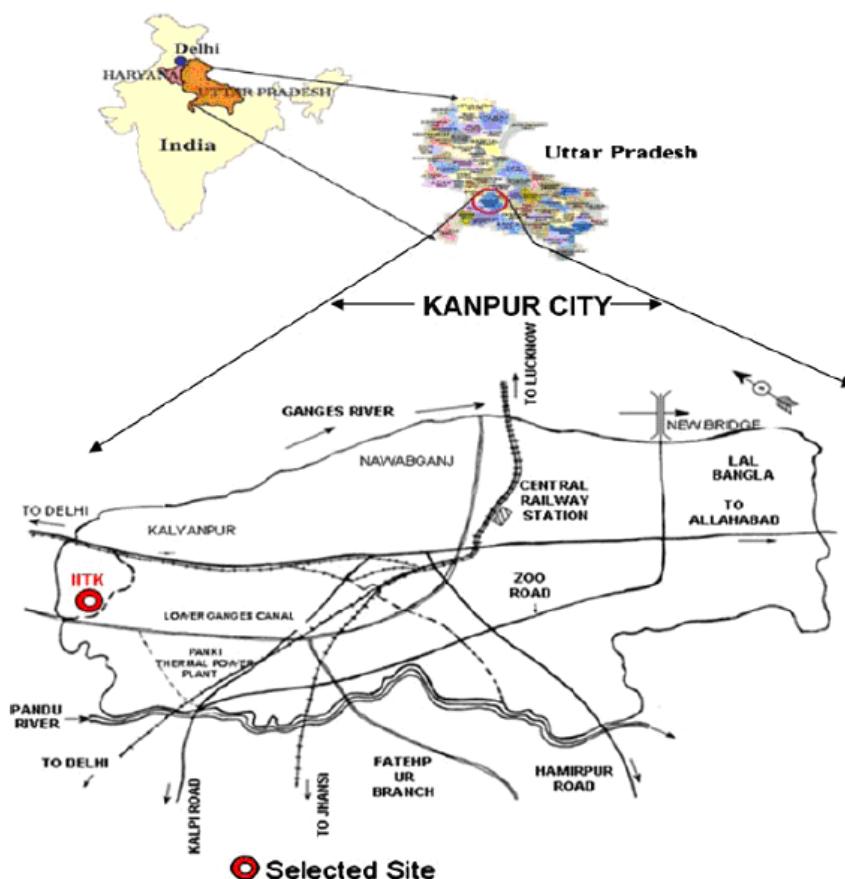


Fig. 1. Location of Kanpur city showing the study site and major sources. After Sharma et al., (2007).

concentration in the diameter range of 15-700 nm, denoted as  $M_{d_{15-700nm}}$  (2) their corresponding size distribution, and (3) BC mass concentration ( $M_{BC}$ ), in Kanpur, an industrial town in the Indo-Gangetic plain. This paper also explores the relationship between these ambient particles' mass concentrations and black carbon, and their association with the prevailing meteorological parameters.

## METHODOLOGY AND DATA

### Site Location

The measurements were made inside the campus of Indian Institute of Technology (IIT), Kanpur. The IIT Kanpur campus, located on the Grand Trunk Road, is about 17 km away from the city center of Kanpur (Fig. 1, after Sharma *et al.*, 2007), where automobiles and a power plant are the principal causes of air pollution, supplemented by biomass burning in winter (Tripathi *et al.*, 2005). The city is mostly encircled by vegetation and agricultural fields. These fields are mostly vegetated in the winter (Nair *et al.*, 2007). The measurement site at IIT is located on the northwest and mostly upwind side of Kanpur (26.43°N, 80.33°E, and 142 m above sea level). The site typically represents the plains of the Ganges basin in the northern part of India. It is worth mentioning the fact that IIT Kanpur has a much cleaner and greener environment compared to the rest of the Kanpur city.

### Experimental Details

Two different instruments were used in this study; namely SMPS and aethalometer. The SMPS was used to measure particle number size distribution, whereas the aethalometer measures BC mass concentration. The SMPS used was a TSI Inc. model 3696, which consists of an electrostatic classifier (model 3080); along with a long differential mobility analyser (long DMA model 3081) and a condensation particle counter (model 3775). The instrument was run with a sheath flow rate of 3.0 L/min (litre per minute) and an aerosol flow rate of 0.3 L/min. A scan time of 150 seconds and retrace time of 30 seconds (3 minutes overall) was employed for each sample, giving a measurable particle size range from 14.6 nm to 697 nm in the long DMA. The data obtained from the SMPS can be retrieved in five different modes—namely number, diameter, area, volume and mass. We retrieved data in the number and mass modes for our study. As recommended by the manufacturer, the mass mode used a particle mass density value of 1.2 g/cm<sup>3</sup> to convert volume to mass. This data recorded every three minutes was grouped on an hourly basis, and thereby reported as an hourly average. The losses of ultrafine particles in the electrostatic classifier of the SMPS near to the inlet are due to diffusion (Baron and Willeke, 2001). These losses occur when the inlet is made of non conductive material. The error also occurs in the CPC due to particle coincidence when the particles number density is above 10<sup>4</sup> #/cm<sup>3</sup>. However, the Aerosol Instrument Manager software rectifies this problem (SMPS manual TSI 3696).

The seven channel aethalometer (AE 41 Magee Scientific, USA) works on the principle of attenuation of the incident light beam, transmitted through the aerosol particles continuously deposited on a quartz fiber filter. Attenuation of light is measured at seven different wavelengths (370 nm, 470 nm, 520 nm, 590 nm, 660 nm, 880 nm, 950 nm) (Hansen *et al.*, 1984). A quartz fiber filter was used to collect the sample, which reduced the scattering of light. The  $M_{BC}$  reported by us was measured at a wavelength of 880 nm. The reason for this choice was that the BC is the principal absorber at this wavelength (Ganguly *et al.*, 2005). The sample flow rate to the aethalometer was 3 L/min at a scan time of 5 minutes. This 5-minute data was averaged on an hourly basis, similar to that done for the SMPS. Uncertainty in the values of BC ranges from 40 to 60 ng/m<sup>3</sup> (Nair *et al.*, 2007) under these conditions. The specific absorption coefficient used is 16.6 m<sup>2</sup>/g

at 880 nm. These values were supplied by the manufacturer, and are also endorsed by Bodhaine (1995).

Meteorological data (temperature and RH) were measured by an automatic weather station (AWS-ES, ISRO20). These were recorded by the instrument as per Greenwich Mean Time (GMT), which was then converted to local time. It was recorded on an hourly basis. The temperature sensors operate with an accuracy of 0.1°C while the accuracy of RH sensor is 2% for RH < 90% and 3% for RH in the range of 90-100% (Tripathi *et al.*, 2005).

The SMPS was placed on the ground floor, inside a double storey building while the aethalometer were placed on the roof of a similar building, about 12 m above the ground with sampling probe extending out of it. The Ganges basin experiences four dominant seasons every year, namely winter (December-February), pre-monsoon (March-May), monsoon (June-August) and post-monsoon (September-November) (Dey *et al.*, 2004; Singh *et al.*, 2004). During the winter season, whole parts of northern India suffer from western disturbances (a series of alternate low- and high-pressure areas), moving from west to east combined with local anthropogenic activity, lead to intense fog and haze in the region (Pasricha *et al.*, 2003). The data collected for the present analysis was divided likewise into foggy, hazy and clear days, which are in turn governed by temperature and RH and number concentration of accumulation mode particles. It was observed by Tripathi *et al.* (2006) that during foggy day particles concentration was higher compared to clear days. Similarly, we also observed that the number density on foggy days was twice that seen on clear days. To further facilitate analysis and assess the effects of various ambient parameters, especially temperature and RH, on the aerosol and black carbon mass concentration (Tripathi *et al.*, 2006); data sets from each season were chosen as follows. At least one graph was chosen which showed the typical diurnal trend in  $M_{d_{15-700nm}}$  and  $M_{BC}$  within a given season, with another day's data being plotted to depict variation from that basic trend, if any. This was repeated for each season.

## RESULTS AND DISCUSSION

The experiments were carried out during the period July 2006 to May 2007. The measurements were taken twice a week, during every week of this period. The results were plotted based on hourly averages, with an error bar indicating variability within that hour. The dotted line plotted vertically across each graph represent sunrise and sunset respectively. In addition, we also plotted an averaged diurnal variation for each season. In this case, the error bars were representative of day to day variability in the dataset.

We selected mass concentration in the size range of 15 nm to 700 nm, which was the measurement window in the SMPS for long DMA, corresponding to the type of impactor and aerosol flow rate fixed by us. Atmospheric BC emitted from combustion process is predominant in the ultrafine mode (Friedlander, 2000; Smith *et al.*, 2005). Therefore fine particles measured by SMPS would include BC too.

The diurnal and seasonal variations of  $M_{d_{15-700nm}}$  and  $M_{BC}$  along with contour plots are shown in Figs. 2-17. We can see a peak in the morning (07:00-09:00 LT) as well as in the evening (20:00-22:00 LT), in all plots except for Fig. 14. It is further observed that the  $M_{BC}$  curve follows a nearly similar trend to that of the curve of submicron aerosol mass and shows a strong correlation. A minimum value of the correlation coefficient was observed on the 2<sup>nd</sup> of August in the monsoon season ( $R = 0.83$ ), the maximum value ( $R = 0.96$ ) being seen on the 9<sup>th</sup> of May in the pre-monsoon. The minimum value of 0.83 could probably be attributed to the fact that data for the whole day was unavailable on the 2<sup>nd</sup> of August. In all the curves we see that, with sunrise, the convective activity rises, leading to a greater level of mixing (Stull, 1988). This helps to lift the fine aerosol particles away

from the earth's surface, thereby; we can see the first peak in the morning. This was followed by a dip at around 14:00 LT in the afternoon, when the boundary layer was the thickest, and the convection was at its maximum. The boundary layer began to thin as the day fell, and so we saw the next peak at night. Furthermore,  $M_{d_{15-700nm}}$  and  $M_{BC}$  show a maximum, whenever there was a minimum in temperature and a maximum in RH, and vice versa. The temperature and RH themselves follow expected opposite diurnal trends, the variability being more pronounced during daytime.

### Monsoon

Fig. 2, which is representative of monsoon, shows the diurnal variation of  $M_{d_{15-700nm}}$  and  $M_{BC}$  on 2<sup>nd</sup> August, 2006. Both follow similar trends, and correlate positively with RH and negatively with temperature. In this season, temperatures vary from 25°C to 35°C. We see a dip in mass concentration at noon, showing increasing trend in the morning and evening. Fig. 2(b) shows that temperature was at a peak value during this time. This suggests that the dip in mass concentration may be caused due to increase in boundary layer thickness.  $M_{d_{15-700nm}}$  and  $M_{BC}$  were low in this season. Also, in this season these particles settle down due to scavenging or wet removal (Friedlander, 2000). In Fig. 3, which represents the size distribution of the same day, there was a high number concentration at around 07:30 LT and again around 21:30 LT. The background concentration of ultrafines was seen to be around 5000 #/cm<sup>3</sup>. Both could be attributed to rush hour traffic, biomass and fossil fuel burning for cooking and heating purposes. The number distribution was seen to be biased more towards the particles in the size bracket below 0.1 μm. Number density of ultrafine range particles usually found near the source is high (Seinfeld and Pandis, 1998). These particles usually comprise of emissions from local combustion sources or atmospheric photochemical activity (Friedlander, 2000). However, chemical analysis data is not available for this season, and we also have not performed the same during our study period, so we cannot exactly quantify any source.

### Post-Monsoon

Fig. 4 shows the diurnal variation of  $M_{d_{15-700nm}}$  and  $M_{BC}$  in the typical post-monsoon season, on 1<sup>st</sup> November, 2006. The temperatures observed in this season were less than those seen in the monsoon, but still showed a clearly pronounced diurnal variation, with a peak at around 14:30 LT. The diurnal variation of RH also was more pronounced this season. The values of  $M_{d_{15-700nm}}$  and  $M_{BC}$  were higher as compared to those seen in monsoon and again, due to traffic there were two peaks at 08:00 LT and 21:00 LT. The valley in both  $M_{d_{15-700nm}}$  and  $M_{BC}$  could be because of increasing thickness of boundary layer in the afternoon. Number size distribution contour plot for the same day is shown in Fig. 5. High number concentrations were observed at 06:30 LT, 12:00 LT and 21:30 LT. The background concentration of ultrafines was seen again to be around 5000 #/cm<sup>3</sup>, with the noontime peak probably because of photochemical activity. Fig. 5 shows a seasonally averaged diurnal variation for post monsoon. The error bars here are characteristic of day to day variability in the hourly averaged values. We see a rather clearly pronounced diurnal variation in the BC mass concentration. A closer look into the diurnal profile of  $M_{d_{15-700nm}}$  betrays that the values of the same actually fall between 11:00 to 17:00 LT, but it is less pronounced as compared to BC. We see a lot of day to day variability in both  $M_{d_{15-700nm}}$  and BC in this season. One reason behind this may be that post monsoon is a transition between monsoon and winter.

### Winter

In the winter season, there exist low temperatures and wind speeds. These parameters inhibit vertical (convective) and

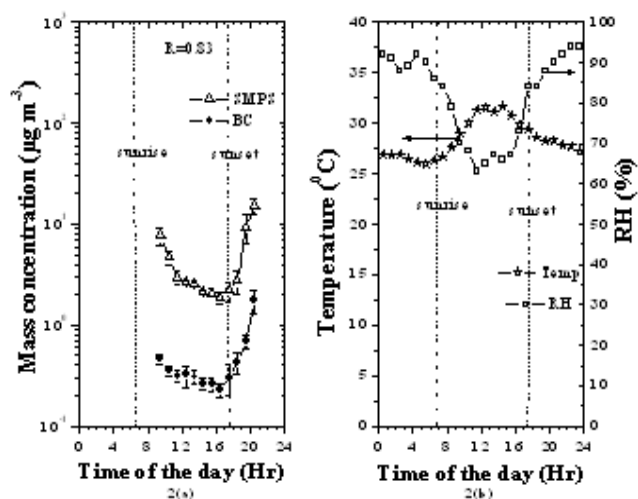


**Fig. 2.** Diurnal variation of black carbon and submicron aerosol mass concentration with temperature and RH, for 2.08.2006. Here, the BC and submicron aerosol mass concentration curves follow same trends. Also, at 14:00 LT, when the temperature shows a maximum, the BC and submicron aerosol profiles show a minimum. After 19:00 LT, the profiles show an upward trend. The vertical lines, as shown in this and later plots, indicates sunrise and sunset times. R is the correlation coefficient between  $M_{BC}$  and  $M_{d_{15-700nm}}$ .

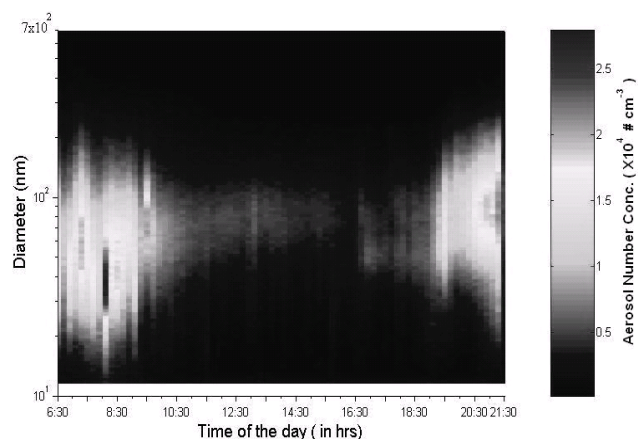


**Fig. 3.** Contour graph for the typical monsoon day, showing the diurnal variation of the number concentration and size distribution on 2.08.2006.

horizontal mixing of aerosols produced at the surface due to the both morning and at night. The first morning peak is due to anthropogenic activity, and enhanced by the fumigation effect. Nair *et al.* (2007) postulated that the boundary layer is quite shallow in the night and early morning and then builds up gradually with the day. In winter maximum BC concentration was confined up to first 500 m above the earth's surface, which is more pronounced in the Forenoon (FN) (68% of the total columnar value), compared to Afternoon (AN) (47%) due to shallow boundary layer. Absolute value of columnar BC at each altitude level is higher during both FN and AN hours of summer compared to winter month; however, the percentage contribution of columnar BC at lower height i.e. up to 500 m, is about 26% higher during FN hour and about 13% higher during AN hour of winter month vis-à-vis summer month (Tripathi *et al.*, 2007). This affects the diurnal variation of the near surface mass concentration. We have classified the winter days into foggy,

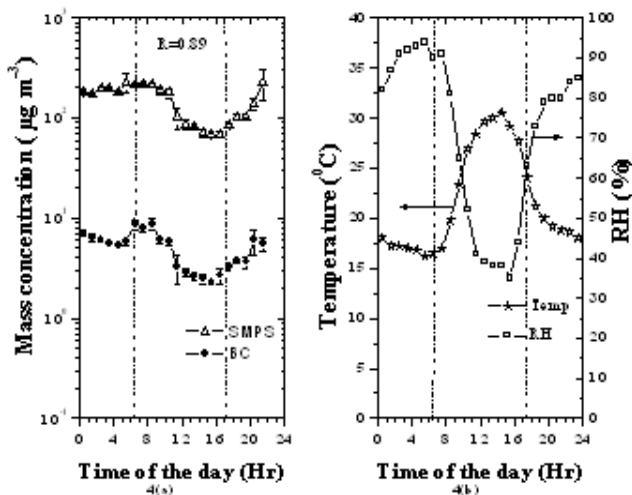


**Fig. 4.** Diurnal variations of BC and submicron aerosol mass concentrations with temperature and relative humidity on 01.11.2006. Both the curves (BC and SMPS) are following same trends. But BC and submicron aerosol mass concentration are very high compared to other dates in the season.

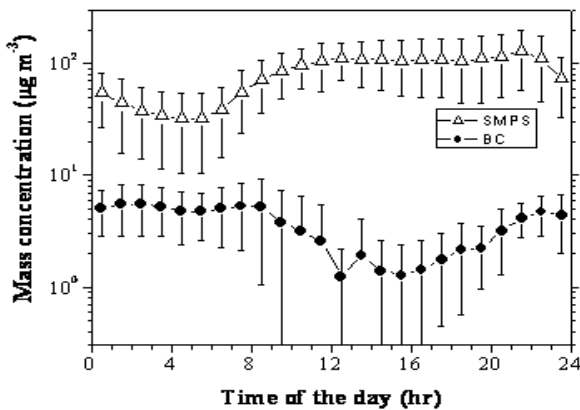


**Fig. 5.** Seasonally averaged diurnal variations of BC and submicron aerosol mass concentrations, for post-monsoon. A closer look into the diurnal profile shows that the profile is flat for BC, whereas, there is a decrease in  $Md_{15-700nm}$  from 11:00 to 15:30 hrs.

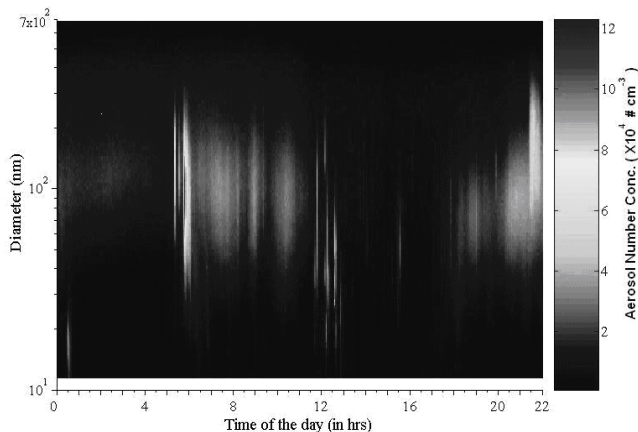


**Fig. 6.** Contour graph for post monsoon season, showing the diurnal variation of the number concentration and size distribution on 01.11.2006.

hazy and clear days, depending upon the prevalent local shallow boundary layer and weak thermal convection (Tripathi *et al.*, 2005). A high mass concentration of aerosol was observed at atmospheric conditions. When there was a dense fog, it was classified as a foggy day. It has been found that a typically dense fog is formed in this region of the Indo-Gangetic plain during winter. One of the factors behind this is the high number of ultrafine aerosols found in the atmosphere. When there was a haze it was termed as a hazy day. A clear day meant a clear sky, with no fog or haze. The background concentration of ultrafine particles was between  $10^4$ - $10^5$   $\#/cm^3$ , an order of magnitude higher vis-à-vis those seen in the other seasons. Also, we see high concentrations of ultrafines during the day in all the seasons, this effect being specially pronounced in the winter. This could be attributed to photochemical activity occurring due to the daytime (McMurry *et al.*, 2005). This is surprising, given that more solar energy is available in the pre-monsoon. The explanation is that anthropogenic activity rises as we move away from the pre-monsoon, and is the most pronounced in the winter. Anthropogenic activity produces a wellspring of semi-volatile organic species, which are the potential precursors for photochemically induced nucleation phenomena (Robinson *et al.*, 2007). The accumulation of these pollutants in the troposphere is also aided by the prevailing meteorological conditions in this season.

#### Clear Winter Days

Figs. 7 and 8 are representative of days on which the sky was clear, with no fog or haze present. On 26<sup>th</sup> January, 2007, two shallow peaks were seen, one at 09:00 LT in the morning, the other at 21:30 LT. Here, we see that the maximum in RH was higher as compared to other seasons and days. Also, the  $Md_{15-700nm}$  and  $M_{BC}$  profiles of these days were flatter compared to other seasons and days, which could be attributed to a thinner boundary layer in the winter. Fig 8 represents the diurnal variation of number distribution for 26<sup>th</sup> January, 2007. It shows that the number concentration was high at midnight, and again at 08:30 LT. We still do not know the reason for high number concentration at midnight, and are still exploring the causes for the same. On these days, it was also observed that the ultrafine particles around 15-20 nm size were present throughout the day. These particles could be emitted from local sources such as anthropogenic activity. The values of  $Md_{15-700nm}$  ranged from 92 to 241  $\mu g/m^3$ , whereas those of  $M_{BC}$  varied from 2.93 to 6.9  $\mu g/m^3$ . Tare *et al.* (2006) did a factor analysis based on 4-stage impactor sampling and subsequent chemical analysis to quantify the sources responsible for fine particle formation in winter. They found that the water soluble species,  $PM_{10}$  and BC were higher on the foggy and hazy days compared to the clear days. They also concluded that during the foggy days, the submicron particles constituted around 81% of the  $PM_{10}$  mass, which was  $232.6 \pm 43.3$   $\mu g/m^3$  on a foggy day against a value of  $175.1 \pm 33.1$   $\mu g/m^3$  on a clear day. They deduced that biomass burning and secondary gas phase reactions contribute most to the fine particle formation.

#### Hazy Winter Days

13<sup>th</sup> January, 2007 was one of the hazy days, depicted in Fig. 9. It shows peaks at 08:30 LT and 21:30 LT, with the peak in  $M_{BC}$  being higher as compared to other seasons and days. The variation in  $Md_{15-700nm}$  was between 29 and 147  $\mu g/m^3$ , whereas that in  $M_{BC}$  was between 1.42 and 6.1  $\mu g/m^3$ , with higher values being seen in the nighttime at around 00:30 LT. The number density of aerosols was higher on hazy days, as compared to clear days. The peaks in  $M_{BC}$  in the monsoon and post monsoon were due to anthropogenic activity (primarily traffic) only. Nair *et al.* (2007) have studied the seasonal variation of black carbon in Kanpur, and found that the BC concentration is higher in winter as compared to other seasons. This is because the anthropogenic

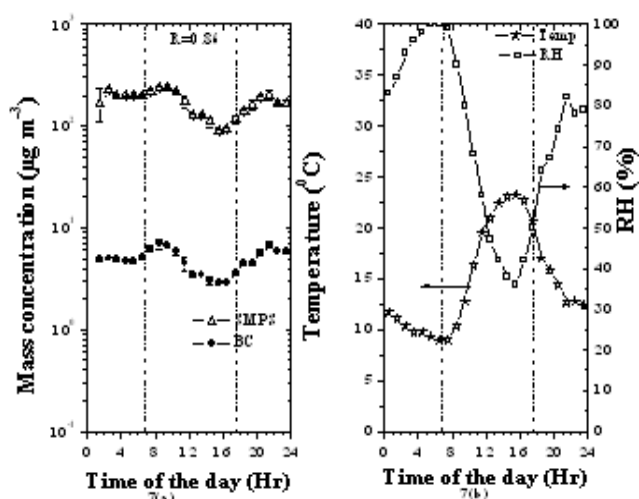


Fig. 7. Diurnal variations of BC and submicron aerosol mass concentrations with temperature and relative humidity on the 26.01.2007. Both the curves (BC and SMPS) are following same trends. There was a shallow peak around 09:30 LT and 21:00 LT. Also, the BC and submicron aerosol mass concentration are higher as compared to other days.

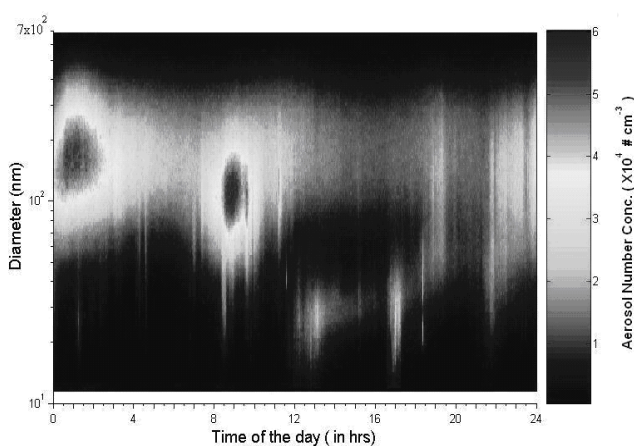


Fig. 8. Contour graph for clear day in winter season, showing the diurnal variation of the number concentration and size distribution on 26.01.2007.

activity rises in winter, (e.g., biomass burning), and also due to the dynamics of the local atmospheric boundary layer (Nair *et al.*, 2007). They observed that in winter, because of low temperatures, there is less turbulence, consequently less mixing and therefore a thinner atmospheric boundary layer. As a result, pollutants are less thoroughly mixed and stay near the surface. It must be noted that this season is characterized by the high frequency of calm conditions, predominant anthropogenic sources, which contain a large fraction of fine particles (Venkataraman *et al.*, 2002).

#### Foggy Winter Days

Fig. 10 is representative of a foggy day showing diurnal variation of  $Md_{15-700nm}$  and BC mass concentrations on 9<sup>th</sup> December for a foggy day. The graphs were nearly parallel and showed strong correlation with temperature and RH. The values of temperature seen in the profiles are lower, and those of RH, are higher, compared to other seasons. The  $Md_{15-700nm}$  varied between 60 and  $175 \mu g/m^3$ , whereas MBC varied between 2.4 and  $4.9 \mu g/m^3$ . We also expressed the size distribution variation of

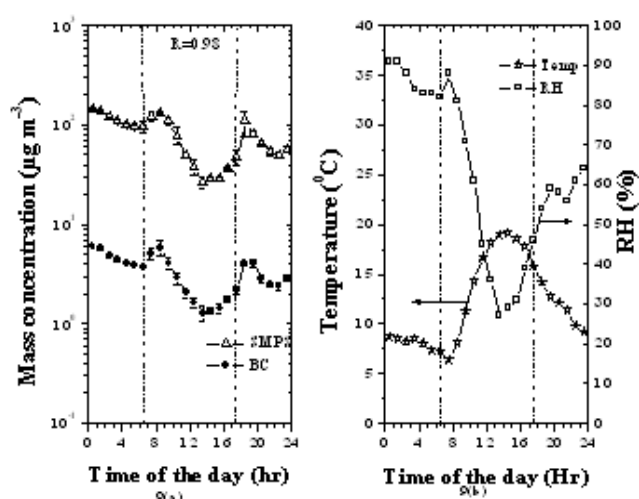


Fig. 9. Diurnal variations of BC and submicron aerosol mass concentrations with temperature and relative humidity on 13.01.2007. Both the curves (BC and SMPS) are following same trends. The BC and submicron mass concentration were high at early morning and all curves show shallow peak around 08:40 LT and 19:30 LT.

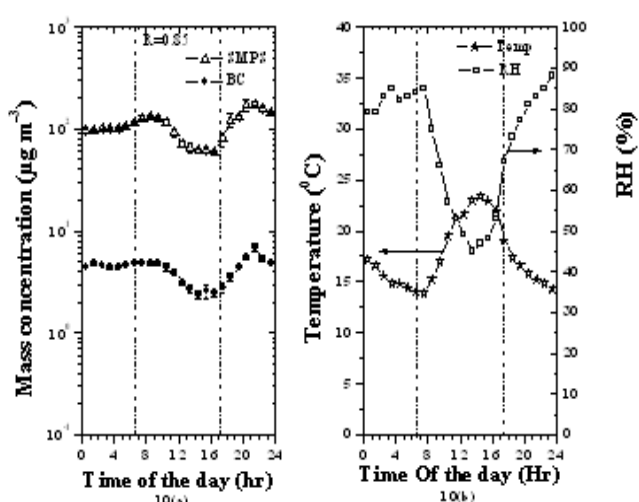
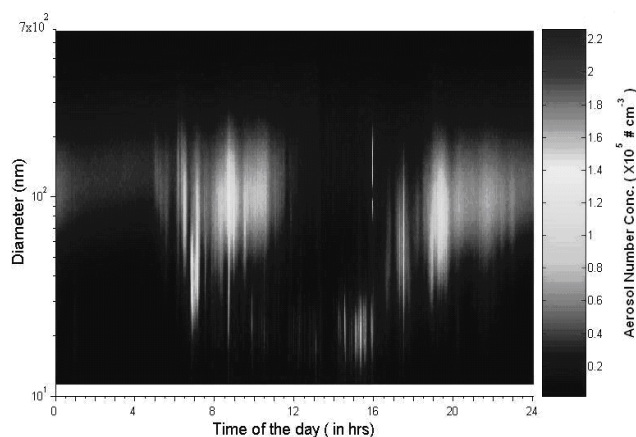


Fig. 10. Diurnal variations of BC and submicron aerosol mass concentrations with temperature and relative humidity on 09.12.2006. Both the curves (BC and SMPS) are following same trends. BC and submicron aerosol mass concentration also increased to one order of magnitude higher than other season. The BC and submicron aerosol mass concentration shows negative correlation with temperature profile. There was a little fog early morning.

25<sup>th</sup> December, 2006, a foggy day, in the form of a contour plot in Fig. 11. This figure shows a maximum in the number distribution at around  $0.1 \mu m$ . The temperature never rose above  $22^\circ C$  during these days. A high number of ultrafine particles less than 20 nm were observed throughout the day. These particles could be from local sources pertaining to biomass combustion and gas phase reaction as delineated in Tare *et al.* (2006), who quantified the sources using factor analysis.

Also, the seasonally averaged diurnal variation for winter is seen in Fig. 12. Again, we see that BC shows a clearer diurnal variation as compared to  $Md_{15-700nm}$ . Also, in the early hours of the day and the late hours of night (00:00-09:00 LT and after



**Fig. 11.** Contour graph for the typical foggy day in winter season, showing the diurnal variation of the number concentration and size distribution on 25.12.2006.

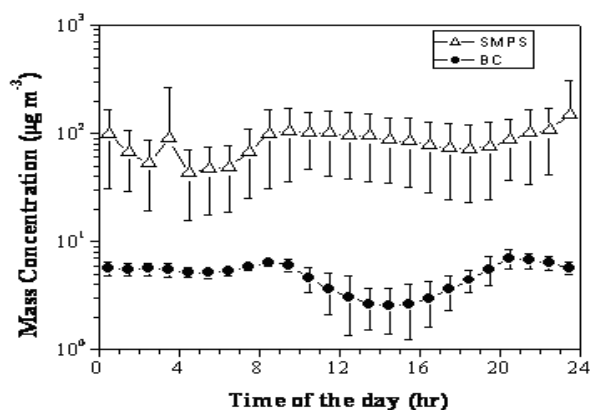


**Fig. 12.** Seasonally averaged diurnal variation of BC and submicron aerosol mass in winter. Error bars represent the day to day variability in the dataset.

19:00 LT), we see smaller error bars in the BC concentration. This may mean that the BC concentration is influenced by sources which vary little day to day, which may include anthropogenic activities like biomass burning and vehicular traffic. On the other hand, a substantial variability is seen in  $Md_{15-700nm}$  which may be attributed to the strongly varying meteorological conditions in this season.

### Pre-Monsoon

The pre-monsoon season was classified into two types: calm day and dust-storm day. During the dust-storm day, the wind speed was nearly 5 m/s. The temperature was also higher as compared to the other seasons, as high as 45°C. Strong dust storm events occur in this region during this season (Dey et al., 2004), which influence the aerosol number size distribution in the accumulation and coarse mode. On the calm day, the  $Md_{15-700nm}$  and  $M_{BC}$  patterns were seen to be congruent. However, this was not so at noon on the dust-stormy day (May 9th), when the two diurnal patterns differed, and showed opposing trends. This was further substantiated by the correlation coefficient between  $M_{BC}$  and  $Md_{15-700nm}$ , which exhibited a negative value of -0.75. We do not know the specific reasons behind this, but it may be due to advection. Also, there might be a lot of non-carbonaceous submicron aerosol present in the dust-storm which may give rise to the phenomena observed. We unfortunately do not have any chemical measurements for a definitive conclusion. The seasonal

average profile is seen in Fig. 15. Again, the trends in BC are more pronounced vis-à-vis  $Md_{15-700nm}$ , with higher variability in the latter. This variability could be attributed to the dust stormy days. Also, after 09:00 LT, we see less variability in the BC values, which may indicate that there is a source whose intensity remains unchanged day to day, namely traffic.

### Analysis of Results

Respective of the season, we see (Figs. 2-17) a fair diurnal variation in both the  $Md_{15-700nm}$  and  $M_{BC}$  mass concentration, and both seem to follow the same trend - high values in the morning and in the night. But this trend was not observed in the averaged profiles, which may be primarily due to variability in the dataset. The BC particles emitted through anthropogenic activity are measured by aethalometer and fall in the ultrafine range, and their mass concentration,  $M_{BC}$  shows strong correlations with the  $Md_{15-700nm}$ . (Smith et al., 2005) The morning peak shows up between 07:00 to 09:00 LT, the night peak between 20:00 to 22:00 LT. The average  $M_{BC}$ , spanning over all three seasons, varied from 0.03-10  $\mu g/m^3$ , which is consistent with the results of Latha and Badarinath (2005) and Bhugwant et al. (2001). We observed the peak in the mass concentration in the morning as well as evening. However, in Figs. 4(a), 7(a) and 9(a) the mass concentration of  $Md_{15-700nm}$  and  $M_{BC}$  was higher in the early morning hours as compared to those at night and could be explained as follows: In the morning, there is an increase in the level of anthropogenic activity such as high traffic, industrial activity and biomass burning for heating purposes (Tripathi et al., 2005), which gives rise to the first peak. Another reason is the residual nocturnal boundary layer, and its associated fumigation effect. At night, all the pollutants come down to the level of the surface. During the daytime, the thickness of the mixed region of the atmospheric boundary layer increases, primarily because of buoyant thermals. Consequently, the pollutants present in the residual boundary layer at night get mixed and dispersed thoroughly, and are carried away from the surface (Stull, 1988). Similarly, at night, the earth's surface cools faster due to radiative cooling thereby change the structure of the atmospheric boundary layer once again. Now, a nocturnal stable layer forms above the ground (Nair et al., 2007). During this season, the boundary layer remains stable upto heights less than 200m from the surface of the earth (Tripathi et al., 2006). This results in a drop in aerosol number, and thereby mass concentration, and the consequent afternoon minima which are seen in all the plots of diurnal variation.

With a few exceptions, the maximum and minimum values for both  $Md_{15-700nm}$  and  $M_{BC}$  increased as one progresses from August, 2006 to January, 2007. This could again be explained by the fumigation effect. In the month of August, the temperature is higher, than in the succeeding months. Consequently, we have a relatively higher degree of turbulence and a higher thickness of mixed boundary layer (Stull, 1988), implying more dispersion, and thereby lower aerosol concentration available to the sampler. As we go towards November through January, one experiences lower temperature and consequently lower turbulence, and thereby lesser thickness of the mixed boundary layer. The wind speed also changed with the season, and was the lowest in winter. Again, an increased level of anthropogenic activity was seen in the winter over the Indo Gangetic Plain, as indicated by a high absorbing index recorded on a Total Ozone Mapping Spectrophotometer (TOMS) (Habib et al., 2006). These effects combined together to give higher values of maxima and minima in winter. We also observed progressively higher number of ultrafine particles during the day, as we approached the month of January (Figs. 7-12) It could be attributed to heterogeneous nucleation persisting throughout the day during the winter season, and also possibly due to high levels of trace gases such as  $NO_x$ ,  $SO_x$  and CO in the winter compared to other seasons (Tare et al.,

2006; Wu et al., 2007). Badarinath et al. (2007) have shown that there is a strong correlation between CO and  $M_{BC}$ , and also between  $O_3$  and  $M_{BC}$  in Allahabad, a city adjacent to Kanpur. They also found that CO and  $NO_x$  concentrations were high during early morning and late evening, when BC concentrations too were high. These trace gases are known to contribute to nucleation in winter.

The diurnal variation of RH has been observed in all the seasons. The RH falls in the afternoon, and rises again in the evening (Figs. 2, 4, 7, 9 and 10). This correlates positively with the aerosol mass. The condensation process is enhanced at higher RH, since it provides a higher driving force for the same. As stated by Friedlander (2000), water forms an important constituent of the accumulation mode aerosol. The water content in these aerosols depends upon the ambient RH.

The size distribution of the aerosol particles change with season, time and other parameters (i.e. temperature and RH). A large number of aerosol particles were found during the day in winter compared to other seasons. Friedlander (2000) stated that the size distribution of the atmospheric aerosol changes with time, the quantitative values changing while the qualitative form of the distribution remained the same. In Figs. 16(a)-16(d), size distribution of aerosol particles are plotted, at time instants corresponding to early morning and late evening peaks in  $M_{BC}$  and  $Md_{15-700nm}$ . Data for size distribution was taken at intervals of 3 min and it was consistent and repeatable. In all the seasons, comparative number size distributions between early morning and late evening were more or less similar, except for the pair in Fig. 16(d). Similar trends have been reported by Whitby et al. (1972) in Los Angeles. In their study, the aerosol number concentration was higher in the morning as compared to other times of the day in the month of September. In our case, we saw the converse, with a clear difference between the values coming on the 9<sup>th</sup> of December. This was a foggy day with low temperature and high RH. It enhances biomass burning, anthropogenic activity and a thinner, mixed boundary layer mass concentration during the mid-day are plotted, for days same as in Fig. 10. Here we did not see any quantitative difference in the size distribution at different times. However we do see bimodal curve on a hazy day in the winter [Fig. 14(c)]. The first peak in the bimodal curve can be attributed to primary particles formed by nucleation. These particles are affected by condensation,

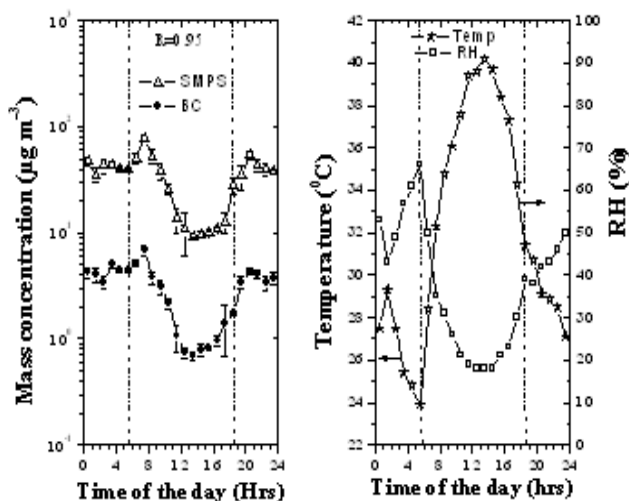


Fig. 13. Diurnal variations of BC and submicron aerosol mass concentrations with temperature and relative humidity on 17.04.2007. Both the curves (BC and SMPS) are following same trends.

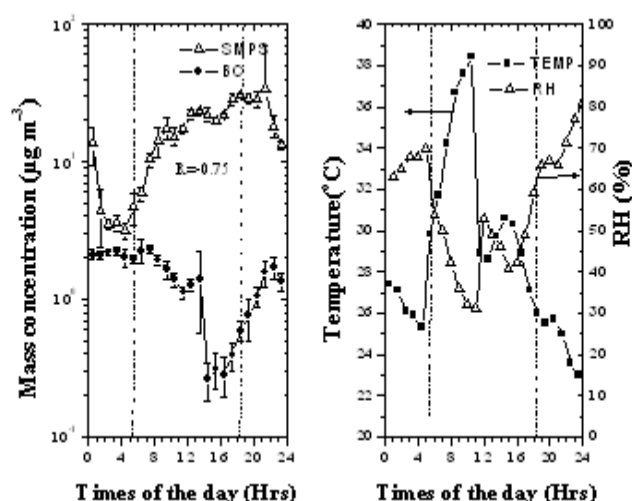


Fig. 14. Diurnal variations of BC and submicron aerosol mass concentrations with temperature and relative humidity on 09.05.2007. Both the curves (BC and SMPS) are not following the same trends because of there was a dust storm event in the afternoon.

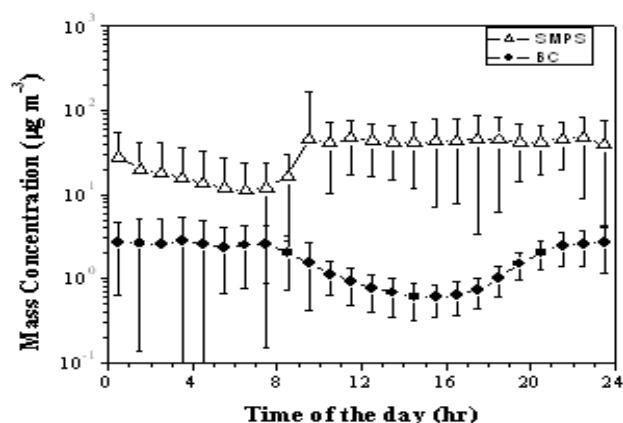


Fig. 15. Seasonally averaged diurnal variations of BC and submicron aerosol mass concentrations for pre-monsoon. Error bars represent the day to day variability in the dataset.

surface reaction and coagulation, which result in the number of ultrafines to fall. This ultimately gives rise to a peak in the accumulation mode (Friedlander, 2000).

Figs. 13 and 14 show the diurnal variation of the aerosol particles in pre monsoon data for calm and dust storm day respectively. The data measured by the two instruments were congruent during calm conditions, but not when there was a dust-storm. The reasons thereof are explained in Section 3.4.

#### Correlations between Different Techniques

Two different measurement techniques and corresponding instruments were used in our study to measure aerosol and black carbon. To compare their predictions and to assess their accuracy, we need to correlate the data that each instrument returns. The observed correlation (Fig. 18) between BC and aerosol mass was calculated based on data from each of the four seasons separately. Each season's hourly  $M_{BC}$  and  $Md_{15-700nm}$  data were taken to this end, giving the fraction of  $M_{BC}$  in  $Md_{15-700nm}$ .

#### (a) Monsoon

From the correlation between BC and  $Md_{15-700nm}$  in the



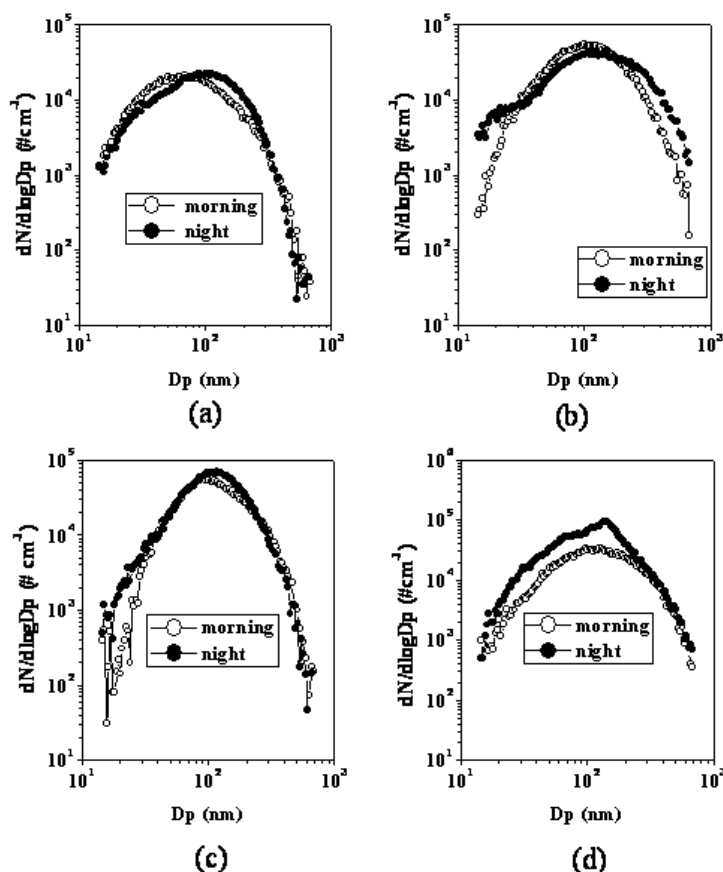


**Fig. 16.** Size distributions of aerosol particles measured by SMPS, peak time of the day at morning and night. Graph represent (a) 2<sup>nd</sup> August, monsoon (b) 21<sup>st</sup> October, post-monsoon (c) 14<sup>th</sup> January, a typical hazy day (d) 9<sup>th</sup> December a typical foggy day.

monsoon season (Fig. 18), we infer that BC occupies approximately 18% of the submicron aerosol mass during the monsoon season. The maximum observed concentration of  $Md_{15-700nm}$  and  $M_{BC}$  mass varied from season to season. The  $Md_{15-700nm}$  and  $M_{BC}$  values measured in the monsoon season varied from 1.86-15.4  $\mu g/m^3$  for  $Md_{15-700nm}$ , while the  $M_{BC}$  values ranged from 0.03-7  $\mu g/m^3$ . The fraction of the black carbon in  $Md_{15-700nm}$  ( $F_{BC}$ ), has also been calculated, and it was observed to be  $0.18 \pm 0.13$  in this season.

#### (b) Post Monsoon

During the post-monsoon season, BC is seen to be about 5% of  $Md_{15-700nm}$ . It is in this season, that the two show the strongest correlation, with an  $R^2$  value of 0.95 in Fig. 18. The  $Md_{15-700nm}$  values ranged from 9.0-227  $\mu g/m^3$  as measured by the SMPS, average  $M_{BC}$  values ranged from 0.561-8.0  $\mu g/m^3$  and  $F_{BC}$  was seen to be  $0.05 \pm 0.01$ .

#### (c) Winter

We see that in the winter, BC mass is about 3% of the submicron aerosol mass. It was observed that the  $M_{BC}$  was higher as compared to other seasons, and ranged from 0.97-9.81  $\mu g/m^3$ . The same could be said regarding  $Md_{15-700nm}$ . Its values, recorded on the SMPS, ranged from 18-388  $\mu g/m^3$ , and  $F_{BC}$  was seen to be  $0.04 \pm 0.01$ . Anthropogenic activity is known to increase as we move towards winter, primarily because of heating purposes. This gives rise to a lot of carbonaceous aerosol. In addition there are no turbulent meteorological conditions (eg., dust storms) which would tend to lower the correlation coefficient.

#### (d) Pre-Monsoon

We observe that in the pre-monsoon season, BC mass is around 8.2% of the submicron aerosol mass, because of the comparatively less number of fine particles in this season. In this season, dust events were observed which dominate the size distribution of the aerosol particles, since dust particles lie in the size window between the accumulation and coarse mode particles. Also,  $F_{BC}$  was seen to be  $0.08 \pm 0.02$ . It was observed that the value of  $F_{BC}$  changed with the season. It was highest in the monsoon and lowest in the winter. This was because BC occupied a large fraction amongst the fine particle mass in the monsoon. In winter, there were other species in addition to the BC, which reduced its share. These species come as a result of increased anthropogenic activity as we move towards the winter season. The predominant ones amongst these are the semi-volatile organic compounds from fossil fuel burning, which give rise to secondary organic aerosols (Robinson *et al.*, 2007).

## CONCLUSIONS

The diurnal and seasonal variations of black carbon (BC) and submicron aerosol mass concentration were studied in Kanpur for four seasons: monsoon, post monsoon, winter and pre-monsoon, using two different instruments-SMPS and aethalometer. Usage of these two in tandem has allowed us to conclude that they give quantitatively close estimates of submicron aerosol and BC mass concentrations, respectively, with the same diurnal pattern. Both BC and submicron aerosol show a peak in concentration twice during the day, the first in the morning between 07:00 and 09:00 LT, and the second in the evening, between 20:00 to 22:00 LT. These occur firstly as a result of increased anthropogenic activities (primarily traffic movement, with an additional load

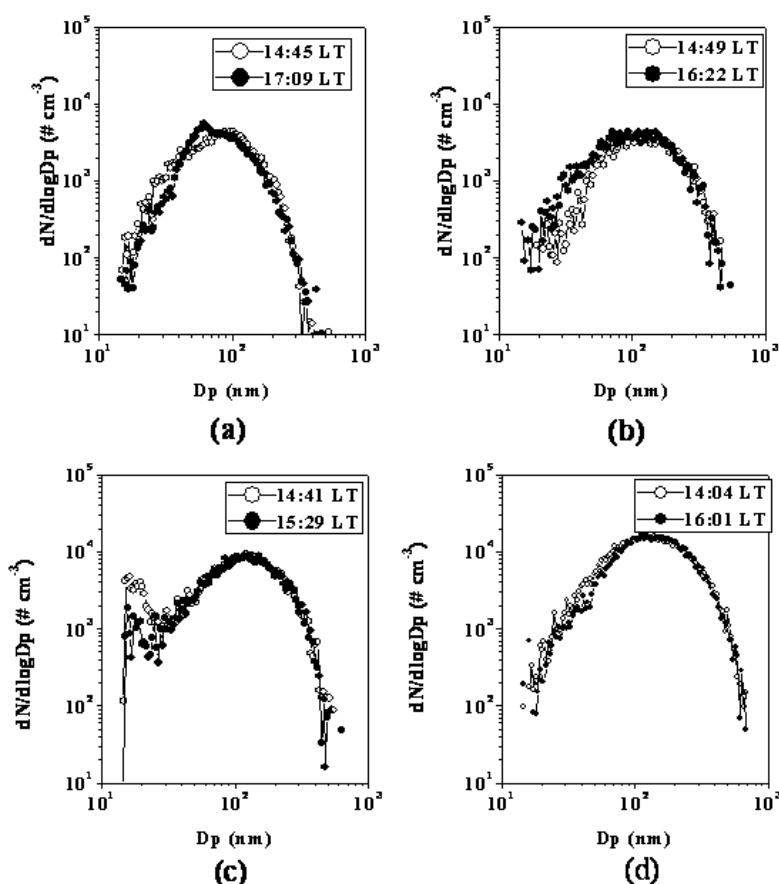


**Fig. 17.** Size distributions of aerosol particles measured by SMPS, at very low aerosol mass concentration was measured during the day. Graph represent (a) 2<sup>nd</sup> August, monsoon , (b) 21<sup>st</sup> October, post-monsoon (c) 14<sup>th</sup> January, a typical hazy day (d) 9<sup>th</sup> December a typical foggy day.

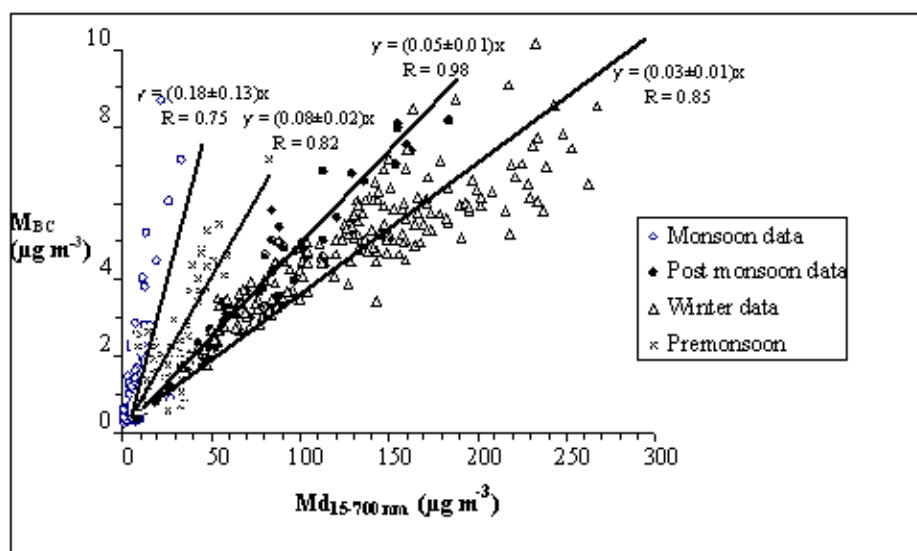


**Fig. 18.** Correlation between the Black Carbon and Submicron Aerosol data: Hourly average BC and submicron aerosol (SMPS) data were taken for each season. R in the above graph is the Pearson correlation coefficient.

due to wintertime biomass burning) and atmospheric boundary layer conditions. The morning peak is also endorsed by the fumigation effect, when the pollutants are being brought near the surface from the residual nocturnal boundary layer (Stull, 1998). The peak concentrations vary from season to season, and were

the highest in winter due to both boundary layer thinning and an increase in the level of anthropogenic activity by enhanced biomass burning. Both the aerosol and BC mass concentrations showed positive correlation with relative humidity (RH) and negative correlation with temperature and these trends could be

explained. The percentage of  $M_{BC}$  in  $Md_{15-700nm}$  varied seasonally, being the highest in monsoon (18%), and lowest in winter (4%), in addition showing a strong positive correlation ( $0.83 \leq R \leq 0.96$ ) between them. These conclusions are valid for all the seasons, except for the times when dust storm occurred; in which case, there was a negative correlation between the two quantities, as depicted in Fig. 14.

The aerosol size distribution from SMPS showed a maximum once in the morning, and once in the night. The size distribution at nighttime was seen to be higher than that observed during daytime, and was the highest on a foggy day. Here, the particle number density was approximately twice that seen on a clear day. In the winter, ultrafine (15-20 nm) particles were observed throughout the day probably because of enhanced photochemical nucleation occurring in this season. In Fig. 16, we see that as we move towards December; difference between the peak values of day and night becomes significant. This is governed by temperature and subsequent anthropogenic activity. In Fig. 14, it is observed that the graphs pertaining to the minima are coincident, except in Fig. 17(c), where a bimodal curve was seen at noon, indicative of a photochemically induced nucleation event. The strongest positive correlation between SMPS and BC data is seen for the post-monsoon season. The fraction of BC in the submicron particles changes with the season, being the highest in the monsoon and lowest in the winter. The low BC fraction in winter shows that there may be other species in the aerosol, like semi-volatile organics, thereby reducing the BC contribution.

#### ACKNOWLEDGEMENTS

One of the authors (SNT) acknowledges the financial support from ISRO Geosphere Biosphere Programme. SNT and RB also acknowledge support from the CARE program, IIT Kanpur, for providing funds for the purchase of the SMPS system.

#### REFERENCES

- Ahamed, Y.N., Arya, B.C., Kumar, A., Shukla, D.K. and Haque, I. (2007). Size Distribution Characteristics of Atmospheric Aerosols over an Urban Site, IASTA Conference, New Delhi, India, 14-17<sup>th</sup> November, 2007.
- Babu, S.S., Satheesh, S.K., and Moorthy, K.K. (2002) Aerosol Radiative Forcing Due to Enhanced Black Carbon at an Urban Site in India. *Geophys. Res. Lett.* 29: 1880.
- Badarinath, K.V.S, Latha, K.M., Chand, T.R.K, Reddy, R.R., Gopal, K.R, Reddy, L.S., Narasimhulu, S.K. and Kumar, K.R. (2007). Black Carbon Aerosols and Gaseous Pollutant in an Urban Area in North India during Fog Period. *Atmos. Res.* 85: 209-216.
- Baron, P.A., and Willeke, K. (2001). An Approach to Performing Aerosol Measurements, in: *Aerosol Measurement: Principles, Techniques and Applications*. 2/e, Wiley Interscience, p.124-126.
- Bhugwant, C., Bessafi, M., Rivieré, E. and Leveau, J. (1995). Diurnal and Seasonal Variation of Carbonaceous Aerosols at a Remote MBL Site of La Réunion Island. *Atmos. Res.* 57: 105-121.
- Bodhaine, B.A. (1995). Aerosol Absorption Measurements at Barrow, Mauna Loa and the South Pole. *J. Geophys. Res.* 100: 8967-8975.
- Bond, T.C. and Bergstrom, R.W. (2006). Light Absorption by Carbonaceous Particles: A Review. *Aerosol Sci. Tech.* 40: 27-67.
- Chu, D.A., Kaufman, Y.J., Zibordi, G., Chern, J.D., Mao, J., Li, C. and Holben, B.N. (2003). Global Monitoring of Air Pollution over Land from the Earth Observing System-Terra Moderate Resolution Imaging Spectroradiometer (MODIS). *J. Geophys. Res.* 108: 4661.
- DeReus, M., Krejcl, R., Williams, J., Fischer, H., Scheele, R. and Strom, J. (2001). Vertical and Horizontal Distributions of the Aerosol Number Concentration and Size Distribution over the Northern Indian Ocean. *J. Geophys. Res.* 106: 28629.
- Dey, S., Tripathi, S.N., Singh, R. P. and Holben, B.N. (2004). Influence of Dust Storms on the Aerosol Optical Properties over the Indo-Gangetic Basin. *J. Geophys. Res.* 119: D20211.
- Dey, S., Tripathi, S.N., Singh, R.P. and Holben, B.N. (2005). Seasonal Variability of the Aerosol Parameters over Kanpur, an Urban Site in the Indo-Gangetic Basin. *Adv. Space Res.* 36: 778-782.
- Friedlander, S.K. (2000). Atmospheric Aerosol Dynamics, in: *Smoke, Dust & Haze: Fundamentals of Aerosol Dynamics*. 2/e, Oxford University Press, p. 359-378.
- Ganguly, D., Jayaraman, A., Gadhavi, H. and Rajesh, T.A. (2005). Features in Wavelength Dependence of Aerosol Absorption Observed over Central India. *Geophys. Res. Lett.* 32: L13821.
- Ganguly, D., Jayaraman, A., Rajesh, T.A. and Gadhavi, H. (2006). Wintertime Aerosol Properties during Foggy and Nonfoggy Days over Urban Center Delhi and Their Implications for Shortwave Radiative Forcing. *J. Geophys. Res.* 111: D15217.
- Gatari, M.J. and Boman, J. (2003). Black Carbon and Total Carbon Measurements at Urban and Rural Sites in Kenya, East Africa. *Atmos. Environ.* 37: 1149-1154.
- Habib, G., Venkataraman, C., Chiapello, I., Ramachandran, S., Olivier Boucher, O. and Reddy, M.S. (2006). Seasonal and Interannual Variability in Absorbing Aerosols over India Derived from TOMS: Relationship to Regional Meteorology and Emissions. *Atmos. Environ.* 40: 1909-1921.
- Hansen, A.D.A., Rosen, H. and Novakov, T. (1984). The Aethalometer – An Instrument for the Real-Time Measurement of Optical Absorption by Aerosol Particles. *Sci. Total Environ.* 36: 191-196.
- Hermann, P. and Hanel, G. (1997). Wintertime Optical Properties of Atmospheric Particles and Weather. *Atmos. Environ.* 31: 4053-4062.
- Hinds, W.C. (1999). Atmospheric Aerosols, in: *Aerosol Science and Technology*, 2/e, Wiley Interscience, p. 304-314.
- Hussein, T., Karppinen, A., Kukkonen, K., Härkönen, J., Aalto, P.P., Hämeri, K., Kerminen, V.M. and Kulmala, M. (2006). Meteorological Dependence of Size-Fractionated Number Concentrations of Urban Aerosol Particles. *Atmos. Environ.* 40: 1427-1440.
- Jacobson, M.Z. (2001). Strong Radiative Heating Due to the Mixing State of Black Carbon on Atmospheric Aerosols. *Nature*. 409: 695-697.
- Kondo, Y. (2006). Temporal Variations of Elemental Carbon in Tokyo. *J. Geophys. Res.* 111: D12205.
- Kothai, P., Saradhi, I.V., Prathibha, P., Hopke, P.K., Pandit, G.G. and Puranik, V.D. (2008). Source Apportionment of Coarse and Fine Particulate Matter at Navi Mumbai, India. *Aerosol Air Qual. Res.* 8: 423-436.
- Kuhlbusch, T.A.J., John, A.C. and Fissan, H. (2001). Diurnal Variations of Aerosol Characteristics at a Rural Measuring Site Close to the Ruhr-Area, Germany. *Atmos. Environ.* 35: 13-21.
- Latha, K.M. and Badarinath, K.V.S. (2005). Seasonal Variations of Black Carbon Aerosols and Total Aerosol Mass Concentrations over Urban Environment in India. *Atmos. Environ.* 39: 4129-4141.
- McMurry, P.H., Finkm, M., Sakurai, H., Stolzenburg, M.R., Mauldin, R.L (III), Smith, J., Eisele, F., Moore, K., Sjostedt, S., Tanner, D., Huey, L.G., Nowak, J.B., Edgerton, E. and Voisin, D. (2005). A Criterion for New Particle Formation in the Sulfur-Rich Atlanta Atmosphere. *J. Geophys. Res.* 110: D22S02.
- Mönkkönen, P., Uma, R., Srinivasan, D., Koponen, I.K.,

- Lehtinen, K.E.J., Hameri, K., Suresh, R., Sharma, V.P. and Kulmala, M. (2004). Relationship and Variations of Aerosol Number and PM<sub>10</sub> Mass Concentrations in a Highly Polluted Urban Environment - New Delhi, India. *Atmos. Environ.* 38: 425-433.
- Moorthy, K.K. et al. (2005). Wintertime Spatial Characteristics of Boundary Layer Aerosols over Peninsular India. *J. Geophys. Res.* 110: D08207.
- Nair, V.S., Moorthy, K.K., Alappattu, D.P., Kunhikrishnan, P.K., George, S., Nair, P.R., Babu, S.S., Abish, B., Satheesh, S.K., Tripathi, S.N., Niranjana, K., Madhavan, B.L., Srikant, V., Dutt, C.B.S., Badarinath, K.V.S. and Reddy, R.R. (2007). Wintertime Aerosol Characteristics over the Indo-Gangetic Plain (IGP): Impacts of Local Boundary Layer Processes and Long-Range Transport. *J. Geophys. Res.* 112: D13205.
- Oberdoster, G. (2001). Pulmonary Effects of Inhaled Ultrafine Particles. *Int. Arch. Occup. Environ. Health.* 74: 1-8.
- Oberdoster, G., Gelein, R.M., Ferin, J. and Weisss, B. (1995). Association of Particulate Air Pollution and acute Mortality: Involvement of Ultrafine Particles? *Inhal. Toxicol.* 7: 111-124.
- Pasricha, P.K., Gera, B.S., Shastri, S., Maini, H.K., Ghosh, A.B., Tiwari, M.K. and Garg, S.C. (2003). Role of the Water Vapor Greenhouse Effect in the Forecasting of Fog Occurrence, Bound. *Boundary Layer Meteorol.* 107: 469-482.
- Prasad, A.K., Singh, R.P. and Kafatos, M. (2006). Influence of Coal Based Thermal Power Plants on Aerosol Optical Properties in the Indo-Gangetic Basin. *Geophys. Res. Lett.* 33: L05805.
- Ramanathan, V. and Ramana, M.V. (2005). Persistent, Widespread, and Strongly Absorbing Haze over the Himalayan Foothills and the Indo-Gangetic Plains. *Pure Appl. Geophys.* 162: 1609-1626.
- Rana, S., Kant, Y. and Dadhwal, V.K. (2009). Diurnal and Seasonal Variation of Spectral Properties of Aerosols over Dehradun, India. *Aerosol Air Qual. Res.* 9: 32-49.
- Robinson, A.L., Donahue, N.M., Shrivastava, M.K., Weitkamp, E.A., Sage, A.M., Grieshop, A.P., Lane, T.E., Pierce, J.R. and Pandis, S.N. (2007). Rethinking Organic Aerosols: Semivolatile Emissions and Photochemical Aging. *Science.* 315: 1259-1262.
- Satheesh, S.K., Moorthy, K.K., Kaufman, Y.J. and Takemura, T. (2006). Aerosol Optical Depth, Physical Properties and Radiative Forcing over the Arabian Sea. *Meteorol. Atmos. Phys.* 91: 45-62.
- Scanning Mobility Particle Sizer<sup>TM</sup> (SMPS<sup>TM</sup>) (2005). Spectrometer Model 3936 Operating and Service Manual, 2005. TSI Inc., USA.
- Seinfeld, J.H. and Pandis, S.N. (1998). Atmospheric Composition, Global Cycles, and Lifetimes, in: *Atmospheric Chemistry and Physics: From Air Pollution to Climate Change*, 2/e, Wiley Interscience, p. 98-101.
- Sharma, M., Kishore, S., Tripathi, S.N. and Behera, S.N. (2007). Role of Atmospheric Ammonia in the Formation of Inorganic Secondary Particulate Matter: A study at Kanpur, India. *J. Atmos. Chem.* 58: 1-17.
- Singh, R.P., Dey, S., Tripathi, S.N., Tare, V. and Holben, B. Variability of Aerosol Parameters over Kanpur, Northern India. *J. Geophys. Res.* 109: D23206.
- Smith, J.N., Moore, K.F., Eisele, F.L., Voisin, D., Ghimire, A.K., Sakurai, H. and McMurry, P.H. (2005). Chemical Composition of Atmospheric Nanoparticles during Nucleation Events in Atlanta. *J. Geophys. Res.* 110: D22S03.
- Srivastava, A., Gupta, S. and Jain, V.K. (2008). Source Apportionment of Total Suspended Particulate Matter in Coarse and Fine Size Ranges over Delhi. *Aerosol Air Qual. Res.* 8: 188-200.
- Stull, R.B. (1988). *An Introduction to Boundary Layer Meteorology*, Kluwer Academic Publishers.
- Tare, V., Tripathi, S.N., Srivastava, A.K., Dey, S., Manar, M., Kanawade, V.P., Agarwal, A., Kishore, S. and Sharma, M. (2006). Measurement of Atmospheric Parameters during ISRO-GBP Land Campaign II at a Typical Location in the Ganga Basin (2006). Chemical Properties. *J. Geophys. Res.* 111: D23210.
- Tripathi et al. (2006). Measurement of Atmospheric Parameters during ISRO-GBP Land Campaign II at a Typical Location in the Ganga Basin: 1. Physical and Optical Properties. *J. Geophys. Res.* 111: D23209.
- Tripathi, S. N., Dey, S., Tare, V., Satheesh, S.K., Lal, S. and Venkataramani, S. (2005). Enhanced Layer of Black Carbon in a North Indian Industrial City. *Geophys. Res. Lett.* 32: L12802.
- Tripathi, S. N., Srivastava, A.K., Dey, S., Satheesh, S.K. and Krishnamoorthy, K. (2007). The Vertical Profile of Atmospheric Heating Rate of Black Carbon Aerosols at Kanpur in Northern India. *Atmos. Environ.* 41: 6909-6915.
- Tripathi, S.N., Dey, S., Tare, V. and Satheesh, S.K. (2005). Aerosol Black Carbon Radiative Forcing at an Industrial City in Northern India. *Geophys. Res. Lett.* 32: L08802.
- Venkataraman, C., Habib, G., Eiguren-Hernandez, A., Miguel, A.H. and Friedlander, S.K. (2005). Residential Biofuels in South Asia: Carbonaceous Aerosol Emissions and Climate Impacts. *Science.* 37: 1454-1456.
- Venkataraman, C., Negi, G., Sardar, S.B. and Rastogi, R. (2002). Size Distributions of Polycyclic Aromatic Hydrocarbons in Aerosol Emissions from Biofuel Combustion. *J. Aerosol. Sci.* 33: 503-518.
- Vinoj, V., Babu, S.S., Satheesh, S.K., Moorthy, K.K. and Kaufman, Y.J. (2004). Radiative Forcing by Aerosols over the Bay of Bengal Region derived from Shipborne, Island-Based and Satellite (Moderate-Resolution Imaging Spectroradiometer) Observation. *J. Geophys. Res.* 109: D05203.
- Weingartner, E., Saathoff, H., Schnaiter, M., Streit, N., Bitnar, B., Baltensperger, U. (2003). Absorption of Light by Soot Particles: Determination of the Absorption Coefficient by Means of Aethalometers. *J. Aerosol. Sci.* 34: 1445-1463.
- Whitby, K.T., Husar, R.B. and Pui, D.Y.H. (1972). The Aerosol Size Distribution of Los Angeles Smog. *J. Coll. Interf. Sci.* 39: 177-204.
- Wu, Z., Hu, M., Liu, S., Wehner, B., Bauer, S., Ma Biling, A., Wiedensohler, A., Petäjä, T., Dal Maso, M. and Kulmala, M. (2007). New Particle Formation in Beijing, China: Statistical Analysis of a 1-Year Data Set. *J. Geophys. Res.* 112: D09209.
- Zhang, Y., Quraishi, T. and Schauer, J.J. (2008). Daily Variations in Sources of Carbonaceous Aerosol in Lahore, Pakistan during a High Pollution Spring Episode. *Aerosol Air Qual. Res.* 8: 130-146.

Received for review, March 18, 2009

Accepted, June 28, 2009